Engineering Ground-Motion Database for Western and Central Australia

Hadi Ghasemi[1] and Trevor Allen[1]

1. Geoscience Australia, GPO Box 378 Canberra ACT 2601 Australia

Abstract

A database of recordings from moderate-to-large magnitude earthquakes is compiled for earthquakes in western and central Australia. Data are mainly recorded by Australian National Seismograph Network (ANSN), complemented with data from temporary deployments, and covering the period of 1990 to 2019. The dataset currently contains 1497 earthquake recordings from 164 earthquakes with magnitudes from M_W 2.5 to 6.1, and hypocentral distances up to 1500 km. The time-series data are consistently processed to correct for the instrument response and to reduce the effect of background noise. A range of ground-motion parameters in the time and frequency domains are calculated and stored in the database. Numerous near-source recordings exceed peak accelerations of 0.10 g and range up to 0.66 g, while the maximum peak velocity of the dataset exceeds 27 cm/s. In addition to its utility for engineering design, the dataset compiled herein will improve characterisation of ground-motion attenuation in the region and will provide an excellent supplement to ground-motion datasets collected in analogue seismotectonic regions worldwide.

Keywords: ground-motion database, waveform processing, engineering parameters

1 Introduction

The aleatory variability within, and epistemic uncertainty between ground-motion attenuation models is often considered to contribute some of the largest uncertainties in probabilistic seismic hazard analyses (Bommer and Abrahamson, 2006; Al Atik *et al.*, 2010). This is particularly true of stable continental region (SCRs) such as Australia with relatively few data recorded from moderate-to-large earthquakes. Nevertheless, ground-motion models (GMMs) that predict the intensity of ground shaking for a given magnitude and distance (on a given site class) form an essential component to modern probabilistic seismic hazard analyses (PSHAs). Whilst there is a paucity of data from which to develop empirical GMMs, stochastic (e.g. Atkinson and Boore, 2006; Liang *et al.*, 2008; Allen, 2012) and physics-based simulation approaches (e.g. Somerville *et al.*, 2009) can be developed through the use of earthquake source and propagation path characteristics from locally recorded data (e.g. Allen *et al.*, 2007). Furthermore, these data may be used for the selection and ranking of appropriate ground-motion models (GMMs) for seismic hazard analysis (e.g. Scherbaum *et al.*, 2009; Ghasemi and Allen, 2018).

This paper describes the compilation of a digital ground-motion dataset recorded from moderate-to-large magnitude earthquakes that have occurred in Proterozoic and Archean terranes of Australian continental crust. It also highlights the procedures employed for consistent correction and processing of time-series data. The computed engineering ground-motion parameters from the high-quality data acquired from recent Australian earthquakes now have significant utility to enable more informed choices for GMMs for future hazard assessments and will support future empirical and simulated ground-motion studies for the nation.

2 Data Compilation

Time-series data have been extracted from continuous waveforms recorded by the Australian National Seismograph Network (ANSN), from various temporary aftershock deployments (e.g. Leonard, 2002; Allen *et al.*, 2019), and from the Incorporated Research Institutions for Seismology (IRIS) data centre. Data from the IRIS data centre have been obtained from three networks: the Australian National Seismograph Network (AU); the Global Seismograph Network - IRIS/USGS (IU); and the Australian Seismometers in Schools (S1) network (Balfour *et al.*, 2014). Additional broadband data from the 2018 Lake Muir earthquake sequence are provided through the University of Western Australia's South West Hub Carbon Capture and Storage Project (Saygin, 2018)

Data from the ANSN are typically streamed at sample rates from 20-40 Hz and high-sample-rate (HSR) data are downloaded on a manual basis following significant earthquakes. This manual download process at Geoscience Australia has been variable over time. Consequently, not all events of interest have these data available. However, where these data are available on local disk storage, HSR data supplant low-sample-rate data from IRIS and the internal continuous waveform buffer. The HSR data are archived in both CSS3.0 and miniSEED format. High-sample-rate data from temporary deployments are archived in PCSUDS and miniSEED format. For the compilation of this dataset, all raw data were first converted to a uniform miniSEED format (Ahern *et al.*, 2007).

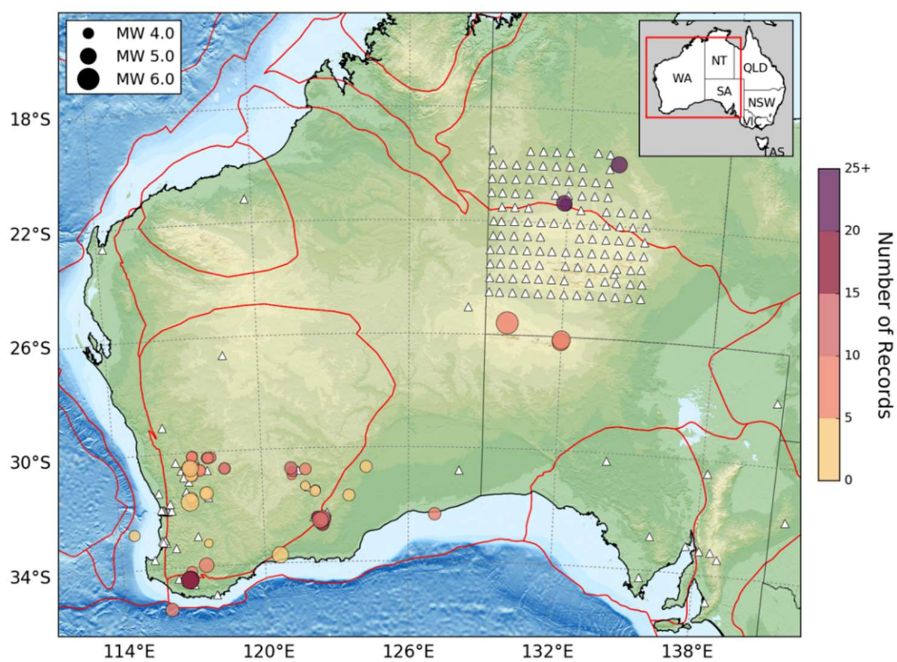

Figure 1. Selected earthquakes, sized by moment magnitude (M_W) and colour-coded by the number of recordings for each earthquake. White symbols indicate the seismic recording stations (from various networks) and the red polygons indicate the neotectonic domains model developed of Clark et al. (2011).

For each recording station, the corresponding instrument transfer function is computed from sensor/digitizer technical specifications (i.e., pole and zero values, and the normalization constant). Such information is either retrieved from IRIS data centre, or, if not available in IRIS, from nominal technical specifications of the sensors deployed at the recording stations of interest. All station metadata, including instrument transfer functions are combined and stored in a standard StationXML format. The compiled inventory for western and central Australia includes 186 stations from five monitoring networks (Figure 1).

The corresponding earthquake information of the collected time-series have been largely taken from existing national catalogues, summarised in the NSHA18 earthquake catalogue (Allen *et al.*, 2018). The primary sources are the Mundaring Geophysical Observatory (MGO) and Geoscience Australia and its predecessors (AUST). Some earthquake locations determined using aftershock deployments have not been translated to the national catalogue. Specifically, these include data from the 2001-02 Burakin (Allen *et al.*, 2006) and 2016 Norseman earthquake sequences. Where available, these updated locations using aftershock deployment data are preferred. Special studies that have carefully relocated some earthquakes have also been included (e.g. Dent and Collins, 2020). The earthquake information, i.e., at minimum location and magnitude in terms of M_W, are first stored in The Quake Markup Language (QuakeML) format.

The compiled time-series data in miniSEED format, station inventory in StationXML format, and earthquake parameters in QuakeML format are then organized and stored in a single, binary database in *Adaptable Seismic Data Format* (ASDF).

3 Data Processing

The collected time-history data are raw data with "count" unit (i.e., the voltage measurement from a sensor). To correct for the instrument response and return the ground-motion in physical unit (e.g., m/s or m/s^2), the instrument transfer function, imported from the database, is deconvolved from the raw time-series to obtain acceleration waveforms in m/s^2. Prior to correcting for instrument response, the baseline of raw data was adjusted by removing the mean followed by 5% cosine tapering. To avoid over-amplification during deconvolving instrument transfer function, the waveform data were also filtered with corner frequencies at 0.001 Hz, and Nyquist frequency. The velocity seismograms were then differentiated to obtain ground acceleration. The acceleration time-series are resampled to 200 sps for consistency and enhancement of temporal resolution.

To account for low- and high-frequency noise, records were padded with zeros, then filtered using acausal, fourth order Butterworth filters. Acausal filters are applied to achieve zero phase shift. Furthermore, unlike causal filters, the computed spectral ordinates within the passband of the acausally filtered accelerations are not sensitive to the filter corner frequencies.

It should be noted that the noise characteristics of each of the ground-motion records is unique and even may vary from one component to another; hence, ideally, each ground-motion record should be filtered with record specific corner frequencies. For each time-series, the corner frequencies of the passband filter are chosen automatically from signal-to-noise ratio (SNR) curve. Record specific SNR curves are computed by dividing the smoothed Fourier Amplitude Spectrum of the signal window with that of the noise window. The passband of the filter is the frequency range in which the SNRs are above 3.0.

Figure 2 shows an example of processed ground-motion record at hypocentral distance of 250 km from an earthquake in Central Australia with M_W 5.0. The Fourier amplitude spectra of signal and noise windows as well as the computed SNR curve are also displayed.

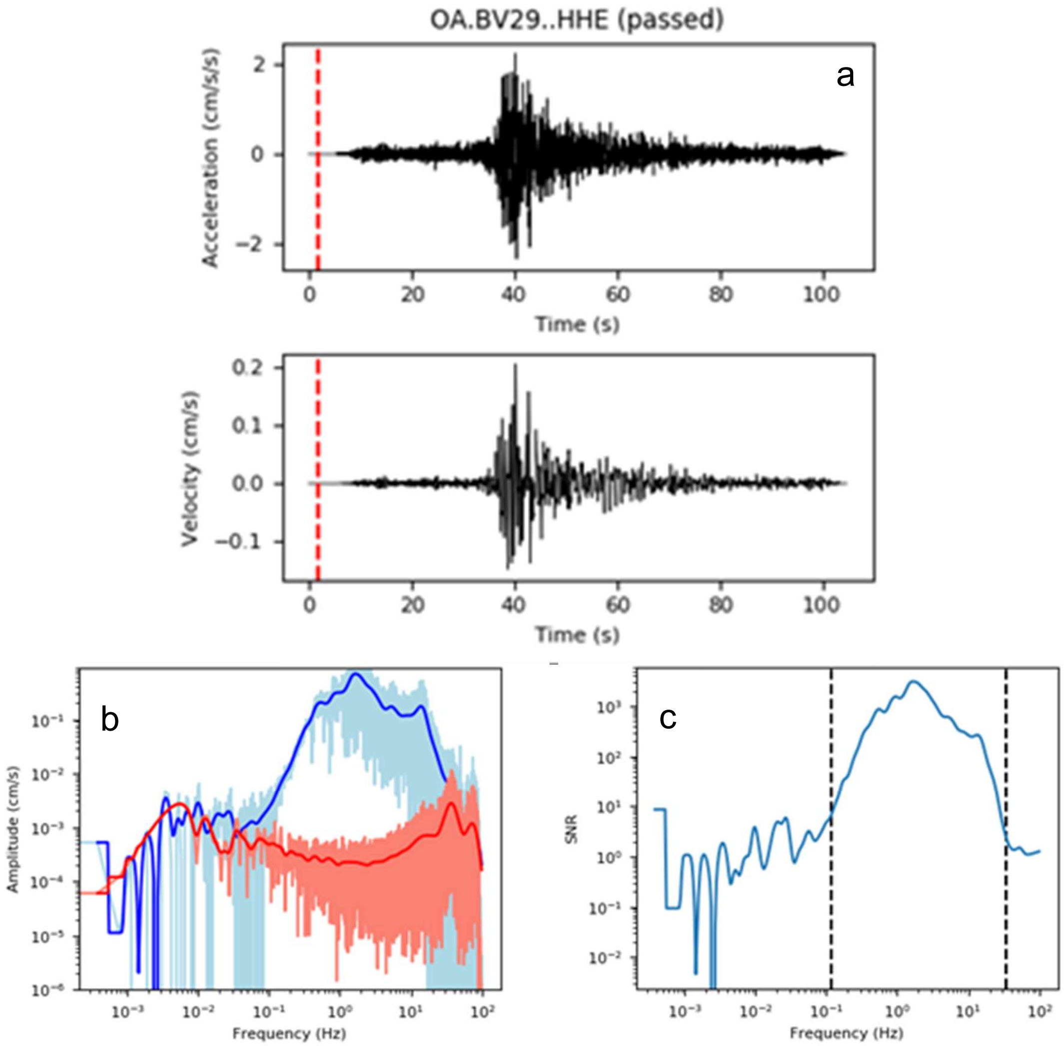

Figure 2. (a) Processed acceleration and integrated velocity time-series recorded at one of the stations deployed as part of the AusARRAY project (Gorbatov et al., 2018). The vertical dashed line indicates the theoretical P-wave arrival time (b) The signal and noise Fourier amplitude spectra, and (c) computed signal-to-noise ratio are also displayed. The vertical dashed lines indicate the selected corner frequencies of the filter.

To define signal and noise windows in an automatic manner for each record, first the theoretical P-wave arrival time is calculated for the observed source-to-site distance based on the IASP91 velocity model. In case of waveforms with timing issues, the theoretical P-wave time may not be within the record time. In such cases, the automatic picker algorithms implemented in ObsPy (Beyreuther *et al.*, 2010) are used to estimate the onset of the P-wave. This P-wave time is then used as the split between the noise and signal windows. The end of the signal window is computed by adding the significant duration of the record to the P-wave time. The significant duration is defined as 5-95% interval of the Arias intensity (Table 1).

Each of the velocity and displacement time-series obtained through integration of the filtered acceleration were visually inspected to check whether or not they appear to be reasonable. The acceleration time-histories that produced unphysical velocity and displacement records were not considered for further processing.

The processed waveforms as well as all of the processing parameters (e.g., filter corner frequencies) are added into the database file in ASDF format.

4 Ground-Motion Parameters

Several engineering ground-motion parameters in time and frequency domains are computed for each of the processed records in the database. Table 1 lists the selected ground-motion parameters along with their definitions. These engineering parameters are widely used to describe the key characteristics of the ground motions and their damage potential. The computed ground-motion parameters are also added into the database.

Table 1: definition of selected ground-motion parameters and their physical units

Parameter	Unit	Definition
Peak ground acceleration	cm/s/s	The largest (absolute) value of ground acceleration
Peak ground velocity	cm/s	The largest (absolute) value of ground velocity
Spectral acceleration	cm/s/s	Maximum acceleration response of a single-degree-of-freedom system to the input ground-motion
Fourier amplitude spectrum	cm/s	The amplitude of the ground-motion with respect to frequency
Arias intensity	cm/s	time-integral of the square of the ground acceleration
duration	s	Total time of ground shaking from P-wave arrivals until the return to background condition

Although the metrics can be accessed directly from the ASDF file, it is also feasible to save the metrics (both station and waveform) into a “flatfile” where each row corresponds to a single record. Such flatfiles can easily be used to study characteristics of the ground motions and develop ground-motion models for seismic hazard studies.

5 Data Summary and Conclusions

This paper describes the compilation of the data and instrument metadata to support the selection and development of GMMs for the seismic hazard assessment for Australia. In total, some 1497 instrument-corrected earthquake recordings are compiled and provided in this dataset. The records are from 164 earthquakes in Western and Central Australia, occurring between 1990 and 2019.The magnitudes of earthquakes within the dataset range from M_W 2.5 to 6.1 and hypocentral distances up to 1500 km. Figure 3 (left) provides a magnitude-distance plot of the compiled data. This data is compared to the magnitude-distance compiled through the Next Generation Attenuation – East project (Goulet *et al.*, 2014), the largest compilation to date of earthquake waveform data for stable eastern North America – a region commonly considered analogous to Australia in terms of its seismotectonic environment. In spite of the limited number of seismic stations located throughout the Australian continental landmass, the dataset compiled herein will provide an excellent supplement to ground-motion datasets collected in analogue seismotectonic regions worldwide.In the compiled database, numerous near-source recordings exceed peak accelerations of 0.10 g and range up to 0.66 g, while the maximum peak velocity of the dataset exceeds 27 cm/s. Figure 3 (right), as an example shows the record section of the processed seismograms of an Mw 5.0 event in Central Australia that is registered by AusARRAY stations. The maximum ground acceleration of 0.013 g is registered at about 43 km away from focal of this quake.

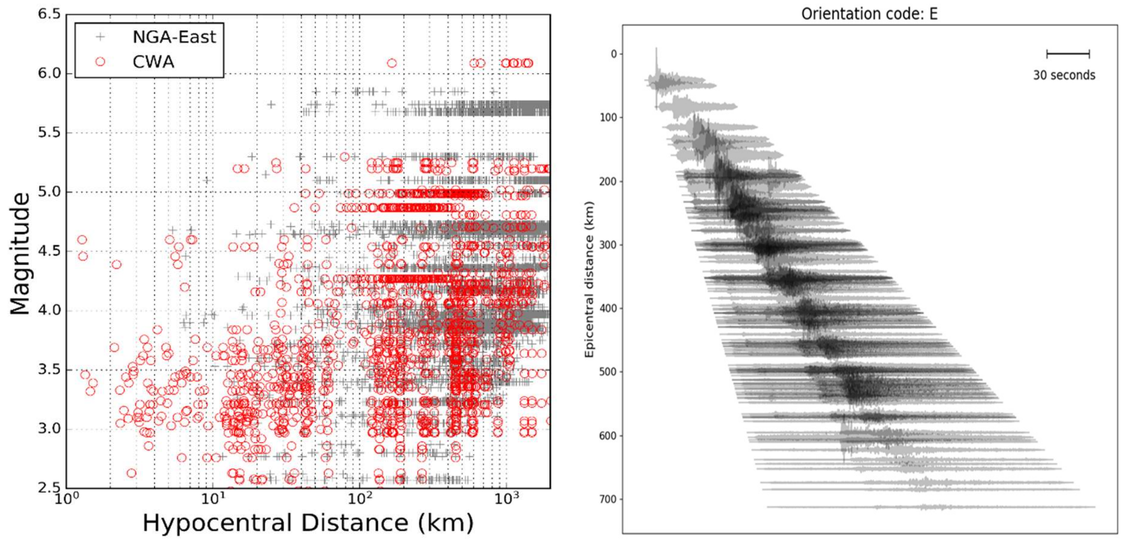

Figure 3. (left) Magnitude-distance distribution of the compiled dataset (CWA) relative to the NGA-East dataset. (right)) Record section of 1 August 2019 M_W 5.0 earthquake near Tennant Creek, Northern Territory.

It is relatively straightforward to compare ground-motion parameters of interest with predictions by GMMs, as the former can be easily accessed by querying the database. Figure 4a, as an example, compares the observed spectral accelerations at 0.2 sec with the model of Allen (2012). The plotted data are from same event as Figure 3.

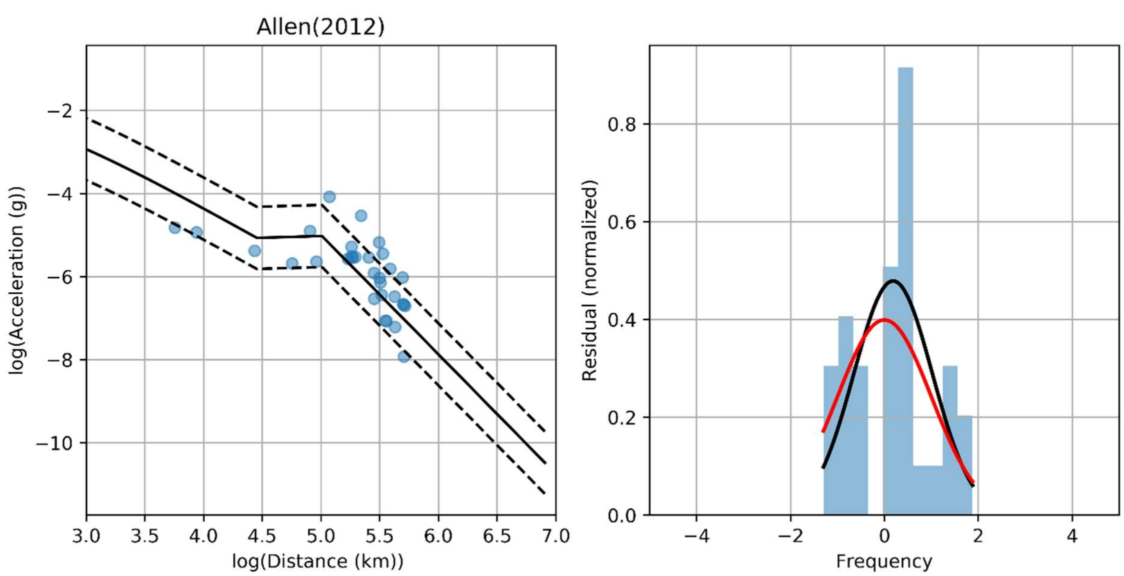

Figure 4. (a) Comparison of the observed spectral accelerations at period of 0.2 sec with the ground-motion model of Allen (2012) for south-eastern Australian earthquakes which assumes a uniform V_{S30} of 820 m/s, (b) Histogram of the normalised residuals. Comparison between fitted normal distribution (black curve) and standard normal distribution (red curve) are also presented. Observations are for the 1 August 2019 M_W 5.0 earthquake near Tennant Creek, Northern Territory.

It can be seen that, overall the Allen (2012; A12) model fits the data reasonably well with most of the observations lie within one standard deviation of the predicted median curve. To further evaluate the fitness of the A12 model, histograms of the normalised residuals are plotted

(Figure 4b). The normalised data residuals should follow the standard normal distribution, i.e., (μ = 0, σ = 1), if data perfectly matches the model predictions. In this figure the standard normal distribution (red curve) is compared with the curve fitted to the normalised residuals (black curve). It can be seen that overall, the A12 model slightly under-predicts the observations, and the scatter in the observations, measured by standard deviation of the fitted normal distribution, is comparable with that from the ground-motion model.

Note that we assumed the local site condition for the Allen (2012) GMM is for "engineering rock" with V_{S30} of 820 m/s, which is similar to average site conditions obtained from geotechnical studies at several seismograph stations across Australia (Collins *et al.*, 2006; Kayen *et al.*, 2014). The local site condition at recording stations remain one of the key missing parameters from the compiled database for Australian earthquakes. McPherson (2017) published a revised seismic site conditions map for Australia based on surficial geology information. This map can provide a good first-order approximation to assess local site conditions of recording stations included in our database. For future work, we also recommend taking advantage of the available seismic waveforms to explore local site characteristics using empirical and theoretical approaches (e.g. Zhao *et al.*, 2006; Kim *et al.*, 2015).

In Geoscience Australia, we are in the process of developing a web interface to allow users to query the database and visualize the waveforms and ground-motion parameters. Database queries would be based on events, stations, and records parameters. The users will be also able to export the data and metadata to standard formats. These data will support the improvement of seismic hazard assessments and will have utility for engineering applications, both in Australia and analogue tectonic regions worldwide.

6 Acknowledgement

Hugh Glanville, Sharmin Shamsalsadati and two anonymous reviewers are thanked for their thoughtful reviews that helped to improve this manuscript. We publish with the permission of the Chief Executive Officer of Geoscience Australia.

7 References

Ahern, T., Casey, R., Barnes, D., Benson, R., and Knight, T. (2007). SEED reference manual, version 2.4, IRIS, 212 pp.

Al Atik, L., Bommer, J., Scherbaum, F., Cotton, F., and Kuehn, N. (2010). The Variability of Ground-Motion Prediction Models and Its Components, *Seismological Research Letters* Vol 81, 10.1785/gssrl.81.5.794.

Allen, T., Clark, D., Lawrie, S., Brenn, G., Dimech, J., Garthwaite, M., Glanville, H., Kemp, T., Lintvelt, C., and Lumley, D. (2019). The 2018 Lake Muir earthquakes: Australia's ninth surface rupturing earthquake sequence in 50 years, *Seismological Research Letters* Vol 90, pp 951.

Allen, T. I. (2012). Stochastic ground-motion prediction equations for southeastern Australian earthquakes using updated source and attenuation parameters, *Geoscience Australia Record 2012/69*, Canberra, 55 pp.

Allen, T. I., Cummins, P. R., Dhu, T., and Schneider, J. F. (2007). Attenuation of ground-motion spectral amplitudes in southeastern Australia, *Bulletin of the Seismological Society of America* Vol 97, No 4, pp 1279-1292.

Allen, T. I., Dhu, T., Cummins, P. R., and Schneider, J. F. (2006). Empirical attenuation of ground-motion spectral amplitudes in southwestern Western Australia, *Bulletin of the Seismological Society of America* Vol 96, No 2, pp 572-585.

Allen, T. I., Gibson, G., Ghasemi, H., and Leonard, M. (2018). *The 2018 National Seismic Hazard Assessment for Australia: Earthquake epicentre catalogue*, Geoscience Australia, pp.

Atkinson, G. M., and Boore, D. M. (2006). Earthquake ground-motion prediction equations for eastern North America, *Bulletin of the seismological society of America* Vol 96, No 6, pp 2181-2205.

Balfour, N. J., Salmon, M., and Sambridge, M. J. S. R. L. (2014). The Australian seismometers in schools network: Education, outreach, research, and monitoring, Vol 85, No 5, pp 1063-1068.

Beyreuther, M., Barsch, R., Krischer, L., Megies, T., Behr, Y., and Wassermann, J. (2010). ObsPy: A Python toolbox for seismology, *Seismological Research Letters* Vol 81, No 3, pp 530-533.

Bommer, J. J., and Abrahamson, N. A. (2006). Why Do Modern Probabilistic Seismic-Hazard Analyses Often Lead to Increased Hazard Estimates?, *Bulletin of the Seismological Society of America* Vol 96, No 6, pp 1967-1977, 10.1785/0120060043.

Clark, D., McPherson, A., and Collins, C. (2011). Australia's seismogenic neotectonic record, *Geoscience Australia Record* Vol 11, pp 1-95.

Collins, C., Kayen, R., Carkin, B., Allen, T., Cummins, P., and McPherson, A. (2006). Shear wave velocity measurement at Australian ground motion seismometer sites by the spectral analysis of surface waves (SASW) method, *Australian Earthquake Engineering Society 2006 Conference*, Canberra, ACT, pp 173-178.

Dent, V., and Collins, C. (2020). The extent of the epicentral zone for events associated with two ML 5 events in March 2002 near Burakin, Western Australia-a review of field and epicentral data, *Proc. AEES 2020, Conference*.

Ghasemi, H., and Allen, T. I. (2018). Selection and ranking of ground-motion models for the 2018 National Seismic Hazard Assessment of Australia: summary of ground-motion data, methodology and outcomes, *Geoscience Australia Record 2018/29*, Canberra, 29 pp, doi: 10.11636/Record.2018.029.

Gorbatov, A., Czarnota, K., and Kemp, T. (2018). Geoscience Australia's contribution to AusArray - Passive seismic imaging of Australia, *ASEG Extended Abstracts* Vol 2018, No 1, pp 1-2, 10.1071/ASEG2018abM1_3G.

Goulet, C., Kishida, T., Ancheta, T., Cramer, C., Darragh, R., Silva, W., Hashah, Y., Harmon, J., Stewart, J., and Wooddell, K. (2014). PEER NGA-East Database, PEER Report 2014/17, Berkeley, California.

Kayen, R. E., Carkin, B. A., Allen, T., Collins, C., McPherson, A., and Minasian, D. (2014). Shear-wave velocity and site-amplification factors for 50 Australian sites determined by the spectral analysis of surface waves method, *U.S. Geological Survey Open-File Report 2014–1264*.

Kim, B., Hashash, Y. M. A., Rathje, E. M., Stewart, J. P., Ni, S., Somerville, P. G., Kottke, A. R., Silva, W. J., and Campbell, K. W. (2015). Subsurface shear-wave velocity characterization using *P*-wave seismograms in Central and Eastern North America, *Earthq. Spectra* Vol.

Leonard, M. (2002). The Burakin WA earthquake sequence Sept 2000 - June 2002, Austrailain Earthquake Engineering Society 2002 Conference. Adelaide, South Australia.

Liang, J. Z., Hao, H., Gaull, B. A., and Sinadinovski, C. (2008). Estimation of strong ground motions in Southwest Western Australia with a combined Green's function and stochastic approach, *Journal of Earthquake Engineering* Vol 12, No 3, pp 382-405.

Saygin, E., and Lumley, D. (2018). Passive seismic investigations at the SW Hub. Perth, Western Australia, University of Western Australia Australian National Low Emissions Council (ANLEC) R&D Project Number 7-0215-0244.

Scherbaum, F., Delavaud, E., and Riggelsen, C. (2009). Model selection in seismic hazard analysis: An information-theoretic perspective, *Bulletin of the Seismological Society of America* Vol 99, No 6, pp 3234-3247.

Somerville, P., Graves, R., Collins, N., Song, S.-G., Ni, S., and Cummins, P. (2009). Source and ground motion models for Australian earthquakes, *Australian Earthquake Engineering Society 2009 Conference*, Newcastle, New South Wales.

Zhao, J. X., Irikura, K., Zhang, J., Fukushima, Y., Somerville, P. G., Asano, A., Ohno, Y., Oouchi, T., Takahashi, T., and Ogawa, H. (2006). An empirical site-classification method for strong-motion stations in Japan using H/V response spectral ratio, *Bulletin of the Seismological Society of America* Vol 96, No 3, pp 914–925, doi: 10.1785/0120050124.